Pharmacological and Kinetic Analysis of K Channel Gating Currents

SHERRILL SPIRES and TED BEGENISICH

From the Department of Physiology, University of Rochester School of Medicine and Dentistry, Rochester, New York 14642; and Marine Biological Laboratory, Woods Hole, Massachusetts 02543

ABSTRACT We have measured gating currents from the squid giant axon using solutions that preserve functional K channels and with experimental conditions that minimize Na channel contributions to these currents. Two pharmacological agents were used to identify a component of gating current that is associated with K channels. Low concentrations of internal Zn^{2+} that considerably slow K channel ionic currents with no effect on Na channel currents altered the component of gating current associated with K channels. At low concentrations (10–50 μM) the small, organic, dipolar molecule phloretin has several reported specific effects on K channels: it reduces K channel conductance, shifts the relationship between channel conductance and membrane voltage (V_m) to more positive potentials, and reduces the voltage dependence of the conductance-V_m relation. The K channel gating charge movements were altered in an analogous manner by 10 μM phloretin. We also measured the dominant time constants of the K channel ionic and gating currents. These time constants were similar over part of the accessible voltage range, but at potentials between −40 and 0 mV the gating current time constants were two to three times faster than the corresponding ionic current values. These features of K channel function can be reproduced by a simple kinetic model in which the channel is considered to consist of two, two-state, nonidentical subunits.

INTRODUCTION

One of the goals of the study of ion channels is to provide a detailed description of the relationship between the structure and the function of these membrane proteins. Such a description for the delayed rectifier K channel is inhibited by the lack of a specific channel ligand that would aid in its biochemical characterization and eventual cloning. Without these types of information, work is often centered on direct measurement of channel function and mathematical modeling to infer molecular details.

One obvious function of the voltage-gated K channel is to provide the efflux of ions from the cell to aid in action potential repolarization. Consequently, the mea-

Address reprint requests to Dr. Ted Begenisich, Department of Physiology, Box 642, University of Rochester Medical Center, Rochester, NY 14642.

J. GEN. PHYSIOL. © The Rockefeller University Press · 0022-1295/89/02/0263/21 $2.00
Volume 93 February 1989 263–283

surement of K channel ionic currents have been much studied. Hodgkin and Huxley (1952*a*) described some of the properties of these currents and developed a mathematical model (Hodgkin and Huxley, 1952*b*) for the channel that could be interpreted in molecular terms.

Hodgkin and Huxley (1952*b*) also predicted that the movement of the charged or dipolar parts of the ionic channels should give rise to gating currents. The characterization of ion channel gating currents is a valuable addition to our understanding of channel function. For example, measurements of Na channel gating currents have been of great importance in suggesting molecular models for Na channel gating (Armstrong and Bezanilla, 1977).

Gilly and Armstrong (1980) reported a component of squid axon gating current that was lost in parallel with the loss of functional K channels that occurs upon exposing axons to K-free internal and external solutions (Chandler and Meves, 1970). Bezanilla et al. (1982) and White and Bezanilla (1985) described methods for reducing Na channel gating currents to improve resolution of the K channel component. They identified a component of gating current with kinetics quite similar to those of K channel ionic currents. These gating currents are altered by conditioning hyperpolarization in a manner analogous to that of K channel ionic currents (Cole and Moore, 1960). Consequently, these currents were identified as arising from K channels. The data obtained by White and Bezanilla (1985) place important constraints on possible models of K channels. They described a model in which the channel was considered to exist in 16 linearly coupled conformations, one of which was conducting.

The methods used by Bezanilla et al. (1982) and White and Bezanilla (1985) included the use of K-free solutions, thus raising the concern that some component of K channel gating current might be lost under such conditions. We report here the measurement of gating currents with solutions that preserve functional K channels. We used pharmacological methods to provide further support for the identification of a component of gating current that can be associated with K channels. We have confirmed the basic observations of White and Bezanilla (1985) but find that the kinetics of the ionic and gating currents are not the same at all potentials. We also present a simple alternative to the 16-state model of these authors. In this model the channel is viewed as consisting of two, two-state independent, nonidentical subunits.

METHODS

Biological Preparation

The data in this report were obtained with giant axons from the squid *Loligo pealei* at the Marine Biological Laboratory, Woods Hole, MA.

Voltage Clamp and Internal Perfusion

The axons used in this study were internally perfused and voltage clamped with techniques that have been previously described in detail (Begenisich and Lynch, 1974; Busath and Begenisich, 1982). Removal of the axoplasm was facilitated by 400–500 μg/ml of the proteolytic

enzyme ficin (Tasaki et al., 1965). Improvements to the electronics allowed essentially complete compensation for the measured series resistance. With these improvements the capacity charging current was complete always within 6 μs and often in less than 5 μs. All voltages have been corrected for the measured junction potential between the internal 0.56 M KCl electrode and the internal solutions used. External potentials were measured with an agar-filled, saturated KCl electrode. Most of gating current measurements were made at 20°C. A few early experiments were done at room temperature, which was 21 to 23°C.

Membrane currents were sampled with a 12-bit analog/digital converter and membrane voltage pulses were generated by a 12-bit digital/analog converter. Both of these units are part of the Scientific Data Acquisition System (Scientific Associates, Inc., Rochester, NY) controlled by an IBM PC/XT computer. The currents were filtered before sampling by a four-pole low-pass Bessel filter at 30 (for ionic currents) or 20 kHz (for gating currents). Before filtering, the membrane current was "blanked" for, usually, 20 μs during each membrane voltage transition. This was done for two reasons: (*a*) This procedure avoided saturation of the various operational amplifiers by the large capacity current transient. (*b*) Since Na channel gating currents are much faster than K channel gating currents, this procedure tends to eliminate much of any residual Na channel gating current. If the current is not blanked, then the filtering tends to distort the fast Na channel gating current and increases the difficulty of separating it from K channel gating current.

A P/4 procedure (Bezanilla and Armstrong, 1977) was used to remove linear leakage and capacitative currents. Unless otherwise noted, gating currents were obtained with a holding potential of −62 mV and the subtracting (P/4) pulses were made from a potential of −102 mV. The recorded gating currents were averages of 32 sweeps. Most recorded ionic currents were the average of two to four sweeps using a −P/4 procedure from the holding potential.

Solutions

Several different external solutions were used in the experiments reported here. These include artificial sea water (ASW) that contained (in millimolar): 440 NaCl, 10 $CaCl_2$, and 50 $MgCl_2$; 50 K ASW: 390 NaCl, 50 KCl, 10 $CaCl_2$, 50 $MgCl_2$; and Tris NO_3 ASW: 416 TrisNO_3, 24 Tris base, and 50 $Ca(NO_3)_2$. ASW and 50 K ASW were buffered to pH 7.4 with 10 mM HEPES and had an osmolarity of 960–970 mosmol. The Tris NO_3 solution had a pH of 7.0 and contained either 10 or 50 mM $CsNO_3$ (called 10 Cs Tris NO_3 ASW and 50 Cs Tris NO_3 ASW, respectively) and sucrose to maintain an osmolarity of 970–980 mosmol. The standard internal solutions (SIS) were K SIS: 270 K glutamate, 50 KF, 15 K_2HPO_4, and 390 glycine; and Cs SIS: 270 Cs glutamate, 50 CsF, 360 glycine, and 10 HEPES. These solutions had pH values of 7.4 and osmolarities of 970–980 mosmol.

The measurement of K channel gating current requires the elimination of Na and K channel ionic currents. This was accomplished using Na- and K-free internal and external solutions, usually Tris NO_3 ASW with 1 μM tetrodotoxin (TTX) to block Na channel ionic current and Cs SIS. The use of NO_3^- follows the work of White and Bezanilla (1985), who showed that this anion reduces Na channel gating and ionic current with little or no effect on K channel ionic current. Further reduction of Na channel gating current was made by using 200 μM dibucaine (Gilly and Armstrong, 1980) and a relatively depolarized holding potential (White and Bezanilla, 1985).

It is well known that K channel conductance is irreversibly lost during perfusion with K-free solutions (Chandler and Meves, 1970). Indeed, Gilly and Armstrong (1980) exploited this result to measure a component of gating current that was lost after K-free perfusion. The loss of K channel conductance is much slower in K-free media if the K ions are replaced by

Cs^+. This is true for both internal (Chandler and Meves, 1970) and external solutions (Almers and Armstrong, 1980). For these reasons we used Cs SIS and Cs-containing external solutions. The data of Fig. 1 demonstrate the excellent survival of K channels with these solutions.

One disadvantage of the use of internal Cs is that this cation has a very small but finite permeability through K channels (Chandler and Meves, 1965). Consequently, this limits the accessible voltage range to potentials below $\sim+25$ mV. A very small amount of this ionic current can be seen in Fig. 2 at the largest depolarization. However, because of its small size and slow kinetics (compared with the gating current) this ionic current interfered with gating current measurements only at membrane potentials above $+10$ mV (see Results). This ionic current can be eliminated by 1 mM of the K channel blockers 3,4-diaminopyridine (DAP) or 4-aminopyridine (4-AP). These compounds were used in some experiments but most of the data were obtained without them.

Except where noted, K channel ionic currents were recorded with 50 K ASW (with 1 μM TTX) and K SIS. The elevated external K concentration reduces (but does not eliminate) the effects of the accumulation of K^+ in the periaxonal space surrounding the giant axon (Frankenhaeuser and Hodgkin, 1956; Adelman et al., 1973).

Data Analysis

A quantitative measure of the kinetics of K channel ionic and gating currents was obtained by fitting an exponential function of time to the data. The algorithm used for these nonlinear fits was "simplex" (Caceci and Cacheris, 1984).

One of the useful parameters for analyzing ion channels is the fraction of open channels (f_{open}). This parameter cannot be uniquely determined from macroscopic ionic current, and the accumulation of K^+ in the periaxonal space further complicates its determination. However, an estimate of f_{open} can be made and several methods have been used for this purpose. Gilly and Armstrong (1982) used relative conductance corrected for K^+ accumulation but did not allow for the voltage dependence of the open channel current-voltage relation. White and Bezanilla (1985) also used the Gilly and Armstrong (1982) method but applied a correction term for the open channel current-voltage relation. This requires the tedious procedure of determining an instantaneous current-voltage relation for each test pulse used.

We have chosen an alternative procedure that is easier to use and yields results quite similar to those of White and Bezanilla (1985). This procedure is based on the technique of Noble and Tsien (1969) for measuring the steady-state activation curve for K channels in cardiac Purkinje fibers. A series of membrane depolarizations is given for a duration sufficient to open all available channels at that potential. The magnitude of the current (often called the "tail" current) immediately after repolarization to the holding potential is measured. The magnitude of this current is directly proportional to the number of channels opened by the activating pulse. Consequently, the determination of the instantaneous current-voltage relation is not necessary.

Unfortunately, the magnitude of the tail current will be altered by K^+ accumulation in the periaxonal space. If the concentration of K^+ is known, the tail current can be appropriately corrected. With the elevated external K^+ concentration in our experiments, the tail current at the holding potential (usually -63 mV for ionic current experiments) is inward. We computed an estimate for the K^+ concentration by using the steady-state current during the pulse and the magnitude of the tail current by the method described in Conner and Stevens (1971). Then, since we know the internal K^+ concentration, we can estimate the external K^+ concentration. If it is assumed that the inward tail current is directly proportional to the K^+ concentration (Wagoner and Oxford, 1987), it is easy to correct for accumulation. The tail current is determined by fitting an exponential function of time and using this fit to extrapolate the

current back to the time of repolarization. The data of Fig. 7 were obtained with this method.

Two other parameters of interest are the charge moved during the depolarizing test pulses (the "ON" charge) and after repolarization to the holding potential (the "OFF" charge). White and Bezanilla (1985) showed that the ON charge can be computed either from a fit of a single exponential of time to the K channel gating current or a direct integration of the current record. We have used the former method in these experiments. Likewise, the OFF charge movements were computed from the fitted exponential functions.

RESULTS

The data shown in Fig. 1 illustrate one of the advantages (see Methods) of using Cs-containing internal and external solutions: the preservation of functional K

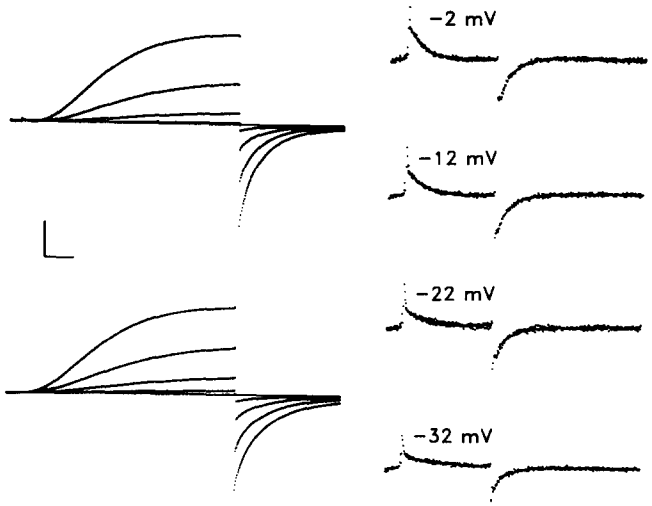

FIGURE 1. K channel ionic and gating currents. (*Left panel*) K channel ionic currents before (upper) and after (lower) recording the gating currents in the right panel. The external solution was 50 K ASW (with 1 μM TTX) and the internal solution was K SIS. The holding potential was −63 mV. The currents shown are those from depolarizations to −43, −33, −23, −13, and −3 mV. The temperature was 15°C. (*Right panel*) Currents recorded in 50 Cs Tris NO_3 ASW and Cs SIS. The holding potential was −62 mV. Currents from 32 depolarizations to −32, −22, −12, and −2 mV were averaged. The temperature was 20°C. Calibration: 0.5 mA/cm^2 (left panel), 15 μA/cm^2 (right panel), 0.5 ms (both).

channels. The upper left panel of this figure shows K channel ionic currents under conditions that are appropriate for these currents. These conditions include a temperature of 15°C, and internal and external solutions containing K.

The currents shown are from depolarizations to −43, −33, −23, −13, and −3 mV. In the right-hand panel are currents recorded with conditions designed to eliminate ionic currents and to produce an enhancement of K channel gating currents over Na channel gating currents as described in Methods. The solutions used are given in the figure legend. The temperature for these records was 20°C. After

recording the gating currents, the temperature was reduced back to 15°C, the K-containing ionic solutions were reintroduced, and the K channel ionic currents of the lower left hand panel were obtained. The K channels clearly survive the perfusion with K-free media quite well.

Gating current records from another axon are shown (points) in Fig. 2 along with the results of fits of exponential functions to the data (solid lines). These functions were fitted to the currents after the test depolarizations (ON's) and after repolarization back to the holding potential (OFF's). The data range used for the fits began shortly after the voltage change (where the solid lines begin) and ended as marked by the arrows. As observed by White and Bezanilla (1985), the single exponential fits are reasonably good representations of the data except for a small, very fast component that is due to residual Na channel gating current.

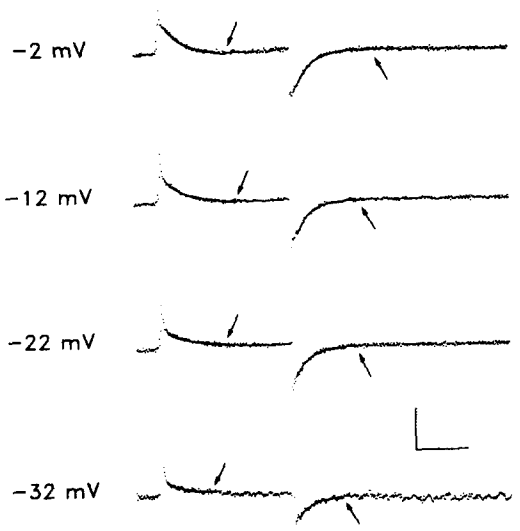

FIGURE 2. Exponential fits to the gating currents. Gating currents measured at the indicated potentials from a holding potential of −62 mV. Fits of an exponential function of time are superimposed (solid line) on the data (dots). The fits were done using data beginning several data points after the change in voltage and ending at the arrows as illustrated. The time constants obtained from the fits to the data at −32, −22, −12, and −2 mV are 0.34, 0.45, 0.39, and 0.36 ms. The time constants from fits to the OFF currents at the holding potential are 0.26, 0.29, 0.27, and 0.29 ms. A fast phase, noticeable during the ON transients, is probably residual Na channel gating current. The temperature was 20°C and there was an average of 32 sweeps. Calibration: 15 $\mu A/cm^2$, 1.0 ms.

The ON time constants, τ_{on}, obtained from the fits at voltages of −32, −22, −12, −2 mV are 0.34, 0.45, 0.39, 0.36 ms, respectively. The OFF time constants, τ_{off}, obtained from the current after depolarizations to these potentials are 0.26, 0.29, 0.27, 0.29 ms. The fact that the τ_{off} values show no consistent change with the size of the preceding depolarization is consistent with the lack of a significant contribution of ionic current to these records.

One of the disadvantages of the use of Cs-containing solutions is the finite permeability of this cation through K channels (see Methods). Some ionic current can be seen in the record of Fig. 2 obtained at −2 mV. This current was negligible at

potentials below +10 mV and, therefore, did not contaminate the gating currents at these potentials. This issue was specifically addressed by recording gating currents from three axons with and without 1 mM 4-AP in the external solution. The ratio of the ON gating current time constants in 4-AP to the values without 4-AP at potentials of −42, −22, −2, and +18 mV were 1.0 ± 0.11 (SEM), 0.98 ± 0.10, 1.03 ± 0.13, and 1.04 ± 0.17, respectively. The ratio of the ON charge moved at these same potentials was 1.03 ± 0.14, 0.97 ± 0.02, 1.04 ± 0.05, and 1.34 ± 0.03, respectively. These data demonstrate no significant effect of K channel ionic current on the determination of gating current time constants. The only effect was the expected underestimate (of ~30%) of ON gating charge at the largest depolarizations. OFF charge movements from these depolarizations determined at the holding potential of −62 mV were not affected because there is no K channel ionic current at this potential.

To justify calling these currents gating currents, it is important to demonstrate that they are due to intramembranous charge movements and are not, for example,

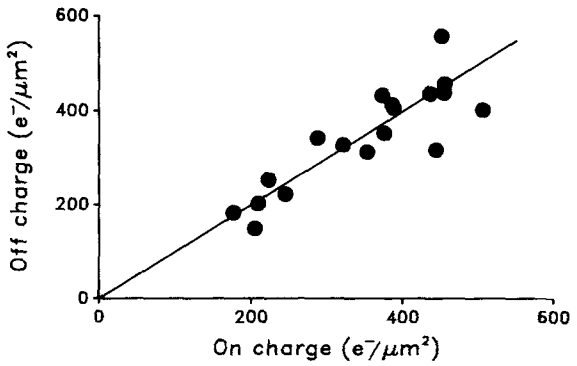

FIGURE 3. Charge moved during ON and OFF transitions. The amount of charge moved during repolarization to the holding potential of −62 is plotted as a function of charge moved during previous depolarizations to −42, −22, −2, and +18 mV. The values of charge movement were obtained from exponential fits to the data as described in Methods. Data from six axons: two with 60 Ca, 10 Cs Tris NO_3 ASW; two with 50 Ca, 10 Cs Tris NO_3 ASW; one with 10 Ca, 50 Mg, 10 Cs Tris NO_3 ASW; and one with 50 Ca, 50 Cs Tris NO_3 ASW. The internal solution was Cs SIS with 200 μM dibucaine. The solid line represents a perfect equality of ON/OFF charge movement. The test pulse duration was either 2.5 or 4 ms. The temperature was 20–23°C.

ionic currents. If these currents result from the movements of membrane-bound charges, then the amount of charge moved after repolarization to the holding potential, Q_{OFF}, should equal the amount of charge moved during the preceding test depolarization, Q_{ON}. A test for the equivalence of Q_{OFF} and Q_{ON} is illustrated in Fig. 3.

In this figure Q_{OFF} values from six axons are plotted as a function of Q_{ON}. Test depolarizations of 2.5 and 4 ms to −42, −22, −2, and +18 mV were used to obtain these data. The solid line represents a perfect equality between the ON and OFF charge movements. There is no systematic deviation of the data from this line of exact equality, which demonstrates that these currents do indeed arise from the movements of intramembranous charges.

Identification of the Gating Currents with K Channels

One of the observations that indicates that most of the gating currents of Figs. 1 and 2 arise from K channel and not Na channel charge movements are the relatively slow kinetics of these currents. Armstrong and Bezanilla (1977) described two phases of Na channel gating current. The slow component has a time constant of ~0.3–0.5 ms at 8°C and is approximately five times slower than the fast Na channel gating current component. Estimates of the Na channel gating current time constant at the warmer (20–23°C) temperatures used here can be made using a Q_{10} value of 3. Such calculations yield values of ~20 and 100 μs for the fast and slow phases, respectively. The time constants obtained in the present study are generally between 200 and 600 μs, much slower than those expected from Na channel gating

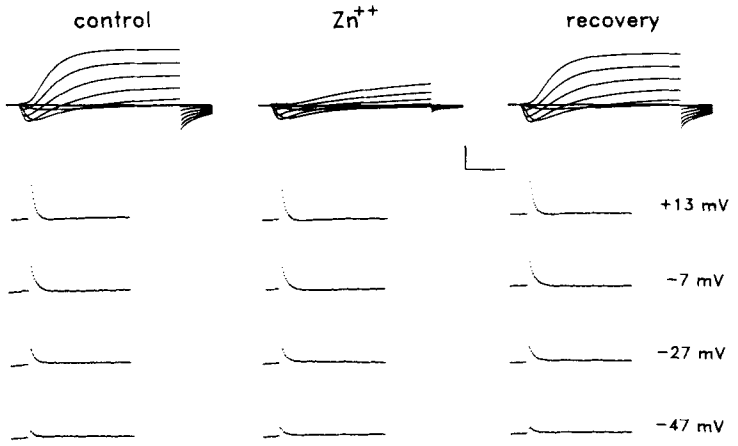

FIGURE 4. Effects of internal Zn on ionic currents and Na channel gating currents. (*Upper panel*) Ionic currents before, during, and after exposure to 3 mM $ZnCl_2$ in K SIS. Currents during depolarizations from −48 to 72 mV in 20-mV steps from a holding potential of −68 mV. The external solution was 50 K ASW. The temperature was 15°C. (*Lower panel*) Na channel gating currents before, during, and after 3 mM $ZnCl_2$ in Cs SIS. Currents recorded at voltages of −47, −27, −7, and + 13 mV from a holding potential of −67 mV. The external solution was ASW with 10 mM Cs and 1 μM TTX. Calibration: 4 mA/cm^2 (upper panel), 40 μA/cm^2 (lower panel), 1.0 ms (both).

currents. Furthermore, Na channel gating currents are reduced ("immobilized") by test pulses of a few ms in duration (at 8°C). The currents described here do not immobilize, as demonstrated by the equality of the Q_{OFF} and Q_{ON} values illustrated in Fig. 3.

It is also possible to distinguish between Na and K channel gating currents with pharmacological methods. Begenisich and Lynch (1974) showed that low concentrations of internal Zn^{2+} specifically affect K channels. This finding is illustrated in the upper panel of Fig. 4. Shown are Na and K channel ionic currents before, during, and after internal perfusion of the axon with 3 mM $ZnCl_2$ in K SIS. (Because of the interaction of Zn^{2+} with F^- and glutamate, the computed concentration of Zn^{2+} is

quite low, ~40 nM; Sillén, 1964). The K channel ionic currents are substantially slowed with little or no change in the Na channel current.

Begenisich and Lynch (1974) also showed that higher concentrations of internal Zn^{2+} do affect Na channel ionic current. Indeed, Bezanilla and Armstrong (1974) used the sensitivity of their measured displacement currents to high concentrations of internal Zn to argue for the association of these currents with Na channels. The lower panel of Fig. 4 demonstrates that the same low concentration (3 mM) of Zn that specifically altered K channel ionic current has a negligible effect on gating currents obtained under conditions designed to emphasize contributions from Na channels (i.e., a lower temperature of 15°C and the absence of dibucaine and NO_3^-). These gating current records were obtained from the same axon that produced the

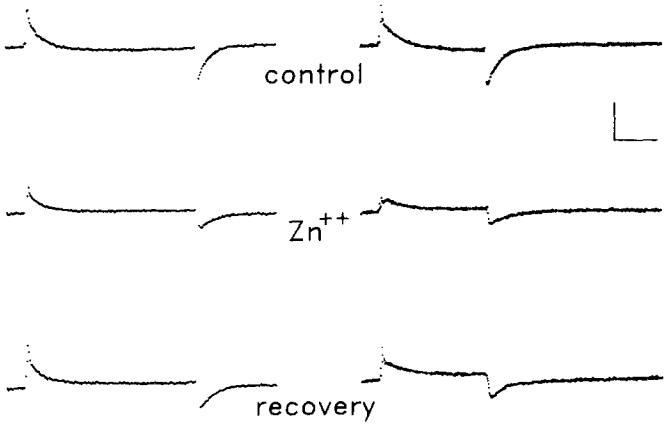

FIGURE 5. Effects of internal Zn on K channel gating currents. K channel gating currents from two different axons (left panel and right panel) at −2 mV are shown before, during, and after treatment with 3 mM Zn in Cs SIS. The holding potential was −62 mV. (*Left panel*) Axon SQDXG, 50 Ca, 10 Cs Tris NO_3 ASW (1 μM TTX and 200 μM dibucaine), with a temperature of 21°C. (*Right Panel*) Axon SQDBV, 50 Ca, 50 Cs Tris NO_3 ASW with 1 μM TTX and 200 μM dibucaine in the internal Cs SIS solution; the temperature was 20°C. Calibration: 25 $\mu A/cm^2$, 1.0 ms.

ionic currents in the upper panel. Under these conditions the gating currents have much faster kinetics than those seen in Figs. 1 and 2 in spite of the colder temperature, which is consistent with their origination from Na channels.

In contrast to the lack of significant effect of internal Zn^{2+} on Na channel ionic and gating currents, the results presented in Fig. 5 show that gating currents measured with conditions designed to enhance contributions from K channels (as in Figs. 1 and 2) are sensitive to low concentrations of this divalent cation. The left and right panels of this figure show gating current from two different axons with similar solutions. Current records elicited by depolarizations to −2 mV are illustrated before, during, and after perfusion with the same internal Zn concentration used in the experiment of Fig. 4. There is a significant effect on the magnitude of the gating

current in both axons. In addition, the faster sampling rate used in the right panel reveals that Zn^{2+} seems to induce (or enhance) a rising phase in the gating current. A more detailed analysis of the actions of internal Zn^{2+} on these currents will be the subject of a future publication. For now, the significant effect of Zn^{2+} on these gating currents supports the view that they arise from K channels.

Another pharmacological compound known to specifically affect K channels is the small, organic, dipolar (at near neutral pH) molecule phloretin. A concentration of phloretin of 10 μM has a negligible effect on Na channels but has several effects on K channels (Strichartz et al., 1980; G. S. Oxford, personal communication). These workers found that the maximum K channel conductance is reduced by ~30%, the conductance-voltage relation is shifted toward more depolarized potentials by ~30 mV and the steepness is reduced, and the ionic current kinetics are slowed by more than a factor of two. All these effects are reversible, though slowly and not always completely.

These actions of phloretin on K channel ionic currents suggest that this compound should also alter K channel gating currents. This is indeed the case, as the results in Fig. 6 illustrate. The top panel of this figure shows the amount of charge movement at several membrane potentials in the absence (open circles) and in the presence (filled circles) of 10 μM phloretin. The lines in this figure are from fits of a function derived from the Boltzmann relation (see Eq. 6) to the data. The fits yield estimates for the maximum charge movement and for the midpoint and steepness of the distribution. This concentration of phloretin reduced the maximum charge movement by 23%, shifted the midpoint of the distribution by 13 mV in the depolarizing direction, and substantially reduced the steepness. The bottom panel shows that the kinetics of the gating current were also affected by phloretin. Illustrated here is τ_{on} at several membrane potentials. Phloretin increased the τ_{on} values at most potentials by as much as a factor of 1.8. These actions of phloretin are quite similar to those on K channel ionic currents and support the notion that these gating currents arise from K channels.

The shift of the midpoint of the Q-V_m relation was much smaller than the reported shift of the K channel conductance-V_m relation (Strichartz et al., 1980). This is only one of several treatments that produced larger effects on K channel ionic currents than on K channel gating currents (Spires and Begenisich, 1985, 1987).

Steady-State and Kinetic Properties of K Channel Ionic and Gating Currents

The upper panel of Fig. 7 shows a comparison of K channel charge movement and the fraction of open channels. Shown are normalized charge movements, Q_{rel}, from five axons. In most cases ON and OFF charge movements were averaged. The method of obtaining these relative charge movements is described in the figure legend. The average fraction of open channels from three of these axons (obtained as described in Methods) is also shown. The lines represent fits of a Boltzmann relation (Eq. 6) to these data. The most noticeable feature of these data is the large separation between the midpoints of these two distributions, which is similar to the observation of White and Bezanilla (1985).

A comparison of the ionic and gating current kinetics is presented in the lower panel of this figure. The kinetics of the ionic currents were obtained by fitting single exponential functions of time to the late part of the current records (from ~50 to ~90% of the maximum value). In agreement with White and Bezanilla (1985) we found a single exponential function to be an excellent fit to this part of the data. The time constants from these fits, τ_K, are plotted as the open symbols. The gating current time constants, τ_g, are shown as filled circles. The ionic current time constant value near −60 mV is from fits to the tail currents; the gating current time

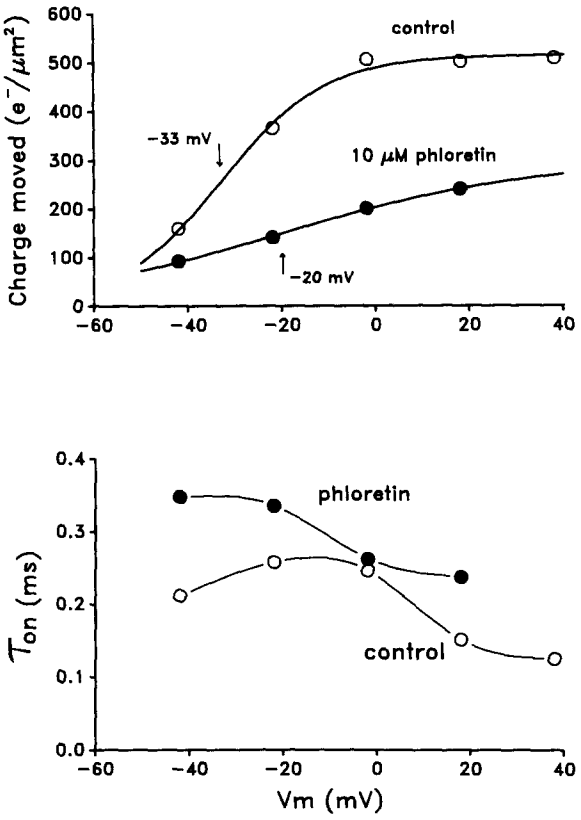

FIGURE 6. Effects of phloretin on K channel gating currents. (*Upper panel*) Charge moved as a function of voltage before (○) and during (●) application of 10 μM phloretin in Cs SIS. The charge moved was obtained from exponential fits to the data as described in Methods. Control: each data point represents the average of the ON and OFF charge movement. The solid line is a best-fit Boltzmann function with a maximum charge movement of 516 $e^-/\mu m^2$ and a midpoint (marked by the arrow) of −33 mV. Phloretin: as for control data, the solid line is the best-fit Boltzmann function with a maximum of 300 $e^-/\mu m^2$ and a midpoint of −20 mV. (*Lower panel*) Effects of phloretin on time constants. Time constants for ON gating currents at several voltages are shown before (○) and during (●) exposure to phloretin. External solution: 50 Ca and 10 Cs Tris NO_3 ASW (1 μM TTX). Internal solution: Cs SIS with 200 μM dibucaine and 1 mM 3,4-DAP. Temperature was 22°C. The solid lines are cubic spline functions used only for connecting the data points.

constant at this potential is the mean of the τ_{off} values. The data of this figure show that the ionic current and gating current time constants are the same at the most negative potentials but diverge substantially at more positive voltages. These values approach each other again at the largest depolarizations.

The aqueous solutions used for determining the ionic current data of Fig. 7 were chosen to optimize the accurate measurement of the ionic currents (as described in

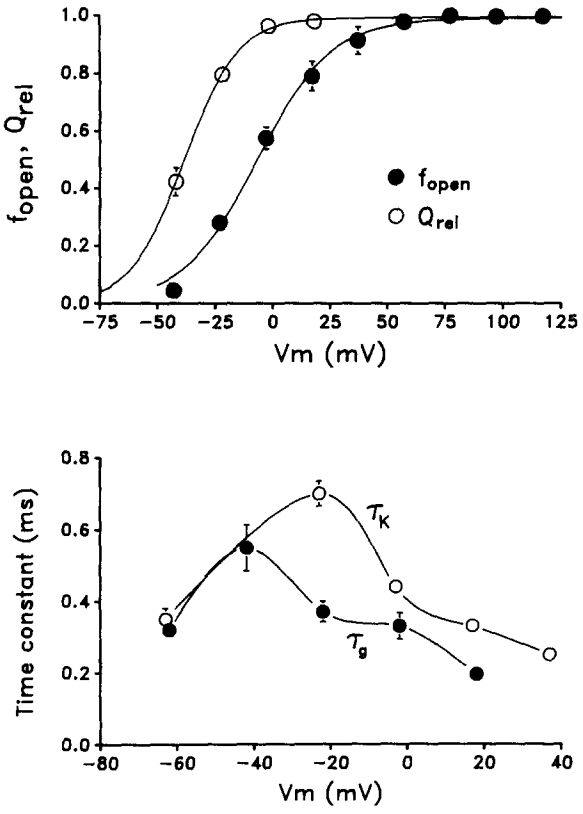

FIGURE 7. Steady-state and kinetic properties of gating and ionic currents. (*Upper panel*) Relative charge movement (○) and fraction of open channels (●) as functions of membrane voltage. The average values of the ON and OFF charge movements from five axons are plotted. The average fraction of open channels (obtained as described in Methods) is from three axons. Charge movements from these three axons are included in the charge movement data. Standard error bars are included if they are larger than the symbols. The ionic currents from which the fraction of open channels was computed were measured with 50 K ASW and K SIS. Three external solutions were used in the gating current experiments: two axons used 60 Ca (0 Mg), 10 Cs Tris NO_3 ASW; two were in 50 Ca (0 Mg), 10 Cs Tris NO_3 ASW; and one with 10 Ca (50 Mg), 0 Cs Tris NO_3 ASW. Cs SIS was the internal solution in all five experiments. As described in the text, the charge-voltage relation of each axon was fit by a Boltzmann function and the charge movement relative to the maximum from the fit was computed. No difference was found with these three solutions. The midpoints of the fitted Boltzmann functions are: −36.4, −40.6, −39.2, −41.4, and −35.4 mV. The q values of Eq. 6 are 2.2, 2.3, 2.0, 1.8, and 2.7. The solid lines are the best-fit Boltzmann functions to these average values. The $V_{1/2}$ value for the charge movement data is −38.4 mV, the q value is 2.2. For the fraction of open channels these parameters were found to be −7.0 mV and 1.6. (*Lower panel*) Ionic and gating current kinetics. Time constants from fits to the ionic current (○) and gating current (●) for the axons of the upper panel are plotted as functions of test potential. The data points at ~−62 mV are from ionic current tails and OFF gating currents. Standard error bars are included if larger than the symbols. The solid lines are cubic spline functions and are used only for connecting the data points.

Methods). Consequently, the ionic and gating current measurements were made with different solutions. To show that the differences in the measured kinetics did not arise from the differences in the solutions, τ_K and τ_{on} were measured from the same axon and with the same external solution. In addition the τ_K values were measured both before and after obtaining the gating current data. As seen in Fig. 8

(upper panel), there is excellent agreement between the τ_K values before and after measuring the gating currents, and these values are almost twice the τ_{on} values.

Several other comparisons of τ_K and τ_g with a variety of external solutions were made. These comparisons are presented in the lower panel of Fig. 8 as the ratio, τ_K/τ_g at several membrane potentials. Over most of the voltage range the ionic currents are substantially (1.5 to almost 3 times) slower than the gating currents. An exception to this occurs at the most negative voltage shown where ionic current tail time constant and τ_{off} values are comparable. There is also the suggestion (seen more clearly in the lower panel of Fig. 7 and the upper panel of Fig. 8) that the ratio may tend closer to unity at positive potentials.

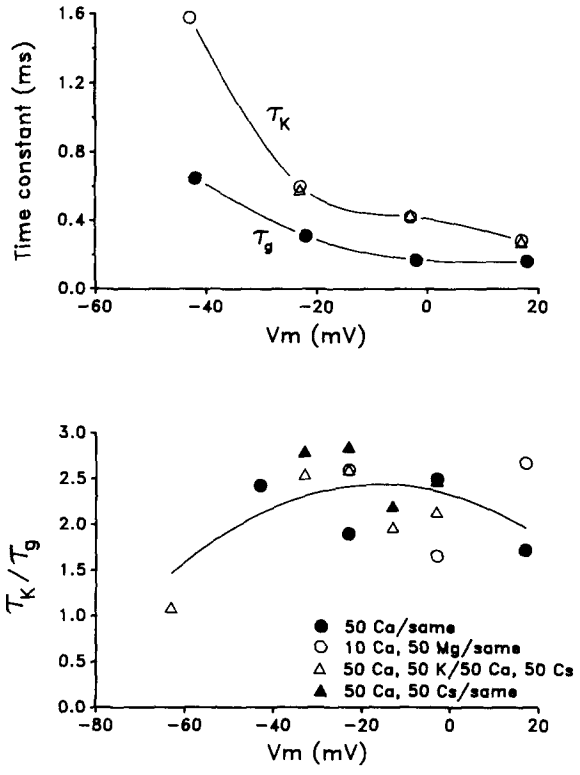

FIGURE 8. Paired comparison of ionic and gating current time constants. (*Upper panel*) Time constant of ionic current, τ_K, before (○) and after (△) measuring gating current time constant, τ_g (●). All measurements were made with the same external solution: 50 Ca, 0 Cs, Tris NO_3 ASW. Ionic currents obtained with K SIS, gating currents with Cs SIS. The temperature was 23°C. The solid lines are cubic spline functions and are used only for connecting the data points. (*Lower panel*) Ratios of τ_K and τ_g from 4 axons in which identical or very similar external solutions were used for ionic and gating currents. This first solution listed in the legend is that used when measuring ionic current, the solution listed after the "/" is that used for gating current measurement. The one point at −63 mV is from the ionic current tail and the gating current OFF time constant at that potential. The temperatures were the same for both ionic and gating current measurements and were between 20 and 23°C. The solid line is a second order polynomial fit to these data.

DISCUSSION

The results presented in this report demonstrate that gating currents can be recorded in K-free solutions and yet preserve K channel function. We showed that the gating currents recorded under conditions designed to minimize contributions

from Na channel currents have pharmacological properties consistent with K but not Na channels. We have also analyzed the kinetics of the K channel ionic and gating currents. We found that the ionic current and gating current time constants were similar over some range of membrane potentials but were a factor of two or more different at other potentials.

Comparison with Previous Results

Gilly and Armstrong (1980) were the first to report a component of squid axon gating current that seemed to be associated with K channels. They exploited the loss of functional K channels that occurs upon exposing axons to K-free internal and external solutions. Bezanilla et al. (1982) and White and Bezanilla (1985) described methods for reducing Na channel gating currents to improve resolution of the K channel component. Their methods included the use of K-free solutions, thus raising the concern that some component of K channel gating current might be lost under such conditions.

We have improved on the methods of these investigators by using solutions that preserve K channel function and by electronically eliminating the fastest part of Na channel gating current from our records. Most of our results are in agreement with those of White and Bezanilla (1985). We have used pharmacological methods to confirm their identification of a significant component of the gating currents as due to the gating of K channels. In agreement with White and Bezanilla (1985), we found a large separation of the Q_{rel}-V_m and f_{open}-V_m relations. While these authors reported a difference of ~40 mV between these relations, our data show a 30-mV displacement. Considering the difficulty in determining f_{open} values and the differences in our methods for so doing, this difference is probably not significant.

Our comparison of the ionic and gating current time constants is somewhat different from those presented by White and Bezanilla (1985). These investigators found that the time constants were quite similar over membrane voltages from ~−100 to −50 mV and from ~0 to +50 mV. At potentials near −60 mV, our data are in complete agreement with these results, and we agree that the time constants tend to be similar (but not identical) at potentials between 0 and 40 mV. We found, however, that the gating current kinetics are substantially faster than the ionic current kinetics in the potential range between −40 and 0 mV. Since White and Bezanilla (1985) did not report values for time constants in this voltage range, our data are not contradictory, but rather supplement their results.

A Qualitative Model

Models of the kinetics of K channels have usually been of two general types: (*a*) those based on the Hodgkin and Huxley (1952*b*) model, which considers the channel to be formed of some number of independent and identical subunits, and (*b*) those that consider the channel to exist in several coupled conformational states. Since 1952, there have been many observations of K channel behavior that are inconsistent with the Hodgkin and Huxley model (see, for example, Cole and Moore, 1960; Palti et al., 1976; White and Bezanilla, 1985). White and Bezanilla (1985) found it necessary to include 15 sequentially coupled closed states and one open (conducting) state of the K channel to qualitatively account for their measured

K channel ionic and gating currents. The single observation that necessitated so many closed states was the large separation between the Q_{rel}-V_m and f_{open}-V_m relations (see Fig. 7, upper panel). We have found that a much simpler model can reproduce this and most other observations of K channel function.

We consider the K channel to be composed of two independent, but not identical, subunits. These subunits can each exist in two conformations, labeled 1 and 2 for one subunit and A and B for the other. The transitions between the conformations are governed by voltage-dependent rate constants:

$$1 \underset{\beta_1}{\overset{\alpha_1}{\longleftrightarrow}} 2$$

$$A \underset{\beta_2}{\overset{\alpha_2}{\longleftrightarrow}} B$$

The rate constants α_1 and α_2 control the transition from state 1 to 2 and from A to B, respectively. β_1 and β_2 are the reverse rate constants for the $2 \rightarrow 1$ and $B \rightarrow A$ transitions.

In this model a channel can conduct only if the subunits are in the 2 and B states. For a population of such channels the fraction of open channels is given by:

$$f_{open} = P_2 \cdot P_B, \tag{1}$$

where P_2 and P_B are the probabilities of the subunits being in states 2 and B, respectively.

The time dependence of these probabilities has the simple form:

$$\begin{aligned} P_2(t) &= P_2^{ss} - (P_2^{ss} - P_2^0) \exp(-t/\tau_{12}) \\ P_B(t) &= P_B^{ss} - (P_B^{ss} - P_B^0) \exp(-t/\tau_{AB}) \end{aligned} \tag{2}$$

where P_2^{ss} and P_B^{ss} denote the steady-state probabilities and P_2^0 and P_B^0 represent the initial values. The time constants are functions of the rate constants:

$$\tau_{12} = 1/(\alpha_1 + \beta_1) \qquad \tau_{AB} = 1/(\alpha_2 + \beta_2) \tag{3}$$

The steady-state values of the probabilities are also functions of the rate constants:

$$P_2^{ss} = 1/(1 + \beta_1/\alpha_1) \qquad P_B^{ss} = 1/(1 + \beta_2/\alpha_2) \tag{4}$$

That is, these probabilities depend only on the ratios of the forward and backward rate constants.

If the voltage dependence of the rate constants is assumed to derive from a movement of charge when the subunits change conformation, the Boltzmann equation can be used to provide the following expressions for the ratio of rate constants:

$$\begin{aligned} \beta_1/\alpha_1 &= \exp\{-[q_{12}(V_m - V_{12})F/RT]\} \\ \beta_2/\alpha_2 &= \exp\{-[q_{AB}(V_m - V_{AB})F/RT]\} \end{aligned} \tag{5}$$

where q_{12} and q_{AB} are the amount of charge moved in the $1 \leftrightarrow 2$ and $A \leftrightarrow B$ transitions, respectively. V_m is the membrane potential and V_{12} and V_{AB} are the midpoints of the charge distribution. Combining Eqs. 4 and 5 yields the following expressions

for the voltage dependence of the steady-state probabilities:

$$P_2^{ss} = 1/(1 + \exp\{-[q_{12}(V_m - V_{12})F/RT]\})$$
$$P_B^{ss} = 1/(1 + \exp\{-[q_{AB}(V_m - V_{AB})F/RT]\}) \quad (6)$$

The gating current can be derived from these equations and is the sum of the gating currents from each of the two subunits:

$$I_g = I_g^{12} + I_g^{AB} \quad (7)$$
$$I_g^{12} = (q_{12}/\tau_{12})(P_2^{ss} - P_2^0)\exp(-t/\tau_{12})$$
$$I_g^{AB} = (q_{AB}/\tau_{AB})(P_B^{ss} - P_B^0)\exp(-t/\tau_{AB}) \quad (8)$$

The integral of the gating current is the charge moved. The steady-state amount of charge movement is a function of voltage and depends on the steady-state probabil-

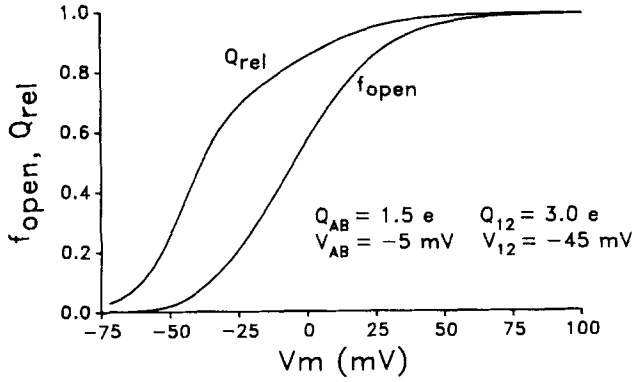

FIGURE 9. Steady-state model parameters. Relative charge movement and fraction of open channels are plotted as functions of membrane voltage. See text for details. Charge moved for the A ↔ B and 1 ↔ 2 transitions are 1.5 and 3 electronic charges, respectively, with midpoints of −5 and −45 mV.

ities P_2^{ss} and P_B^{ss}. The normalized steady-state charge movement, Q_{rel}, is given by:

$$Q_{rel} = (q_{12}P_2^{ss} + q_{AB}P_B^{ss})/(q_{12} + q_{AB}) \quad (9)$$

Computations from this simple model are illustrated in Figs. 9 and 10. The specific model parameters used are given in the figure legends. Fig. 9 shows that this model can reproduce the observed large displacement between the Q_{rel}-V_m and f_{open}-V_m relations. This difference results from the 40 mV separation of the charge distributions from the two model subunits. Consequently, the charge movement at negative potentials is due mostly to the 1 ↔ 2 transition and the charge moved at potentials near 0 mV has a large contribution from the A ↔ B transition. Since the channel is open only if these subunits are in the 2 and the B states, the f_{open} curve reflects the fact that the probability of being in the B state is high only at relatively positive potentials.

The results of computations of the time course of f_{open} (Eqs. 1 and 2) at several potentials are illustrated in Fig. 10 *A*. The ionic currents would have a similar

appearance but would need to be scaled for the appropriate open channel current-V_m relation. As described in the figure legend, the time constants for the 1 ↔ 2 transition were chosen to be those of the measured gating current time constants of Fig. 7 (lower panel). Similarly, the time constants for the A ↔ B subunit were chosen to match those of the ionic current time constants of Fig. 7.

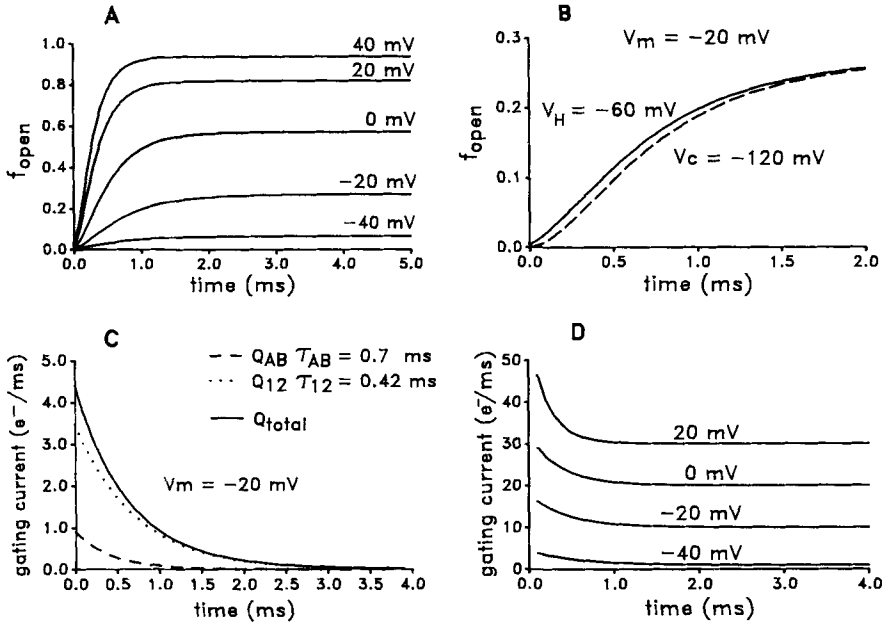

FIGURE 10. Ionic and gating current properties of the model. (*A*) Time course of fraction of open channels at several voltages. The voltage dependence of the fraction of channels open in steady state is as described in the text (and as shown in Fig. 9). The time constants for τ_{12} and τ_{AB} were obtained from the data in the lower panel of Fig. 7. (*B*) Conditioning hyperpolarization induced delay in the opening of channels. The computations for the solid line were done with a holding potential of −60 mV. The test pulse voltage is −20 mV. The dashed line represents computations from a holding potential of −120 mV. (*C*) The two components of the gating current at −20 mV. The dotted line illustrates the gating current for the 1 ↔ 2 transition, while the dashed line illustrates the gating current for the A ↔ B transition. The solid line is the total gating current. (*D*) Gating current time course at several potentials. Steady-state model parameters are as described in the text (and Fig. 9) and are the same as for parts *A* above. Time constants are from data in the lower panel of Fig. 7 and are the same as those in part *A* above. The record for each depolarization has been shifted vertically for clarity.

One of the important properties of K channels is the delay in the time course of the ionic current after a conditioning hyperpolarization (Cole and Moore, 1960). Fig. 10 *B* shows that this simple model exhibits this type of behavior. The model parameters are the same as those used for the computations of Figs. 9 and 10 *A*.

This simple model predicts two temporal components of the gating current, which may, at first, appear contradictory to the quality of single exponential fits to

the gating currents. The results presented in Fig. 10 *C* illustrate that there is, in fact, no contradiction. As shown in this figure, the dominant contribution to the total gating current (solid line) is the contribution from the 1 ↔ 2 transition (dotted line). Gating current from the A ↔ B transition (dashed line) makes a rather small contribution because, as Eq. 8 illustrates, the gating current magnitude involves both the amount of charge moved and the kinetics of the movement. The A ↔ B transition involves half the amount of charge of the 1 ↔ 2 transition and has kinetics almost a factor of two slower. This results in a weighting factor (see Eq. 8) of almost a factor of four for gating currents from the 1 ↔ 2 subunit. This smaller, slower component would be difficult to resolve experimentally.

Fig. 10 *D* shows the computed gating currents at several potentials. As described for Fig. 10 *C*, the model τ_{12} values were chosen as the τ_g values of Fig. 7 (lower panel) and τ_{AB} as τ_K. These currents are generally similar to the measured gating currents of Figs. 1, 2, and 4 (left panel).

The independent nature of the two subunits allows the possibility that drugs or chemical reagents might alter K channel gating and ionic currents in different ways or to different degrees. Perhaps this explains the phloretin data in Results and the results of some amino acid reagents (Spires and Begenisich, 1985, 1987). A quantitative analysis of this suggestion is beyond the scope of this report and is the subject of ongoing investigations.

In summary, this simple, two-independent-subunits model for K channels reproduces qualitatively many of the important observations of K channel function. It exhibits the observed large separation between charge movement and the fraction of open channels (Fig. 7, upper panel, and Fig. 9). It predicts a delay of the ionic current due to conditioning hyperpolarization seen in K channels (Cole and Moore, 1960; Fig. 10 *B*). This simple model also can account for the difference between the measured ionic and gating current time constants (Fig. 7, lower panel, and Fig. 8). This difference occurs because the gating currents are dominated by steps in the channel conformational change process that involve large amounts of charge movements with fast kinetics (Eq. 8 and Fig. 10 *C*).

Limitations of the Simple Model

The model described above can qualitatively account for all the observations in this report and other observed features of K channel function. It does this as well as the model described in White and Bezanilla (1985), but without the complexity inherent in the 16 conformational states of that model. However, there are several deficiencies of this simple model. The most important of these is that White and Bezanilla (1985) observed that, under suitable conditions, the K channel gating current exhibits a rising phase. We have also observed this behavior under similar conditions and after treatment with internal Zn^{2+} as shown in Fig. 5 (right panel). The simple model does not exhibit a rising phase. Also, the model Q_{rel}-V_m relation (Fig. 9) at potentials between ~ -20 and 0 mV is not in quantitative agreement with the measured data in Fig. 7 (upper panel). Finally, the sigmoid time course of K channel ionic current, especially after conditioning hyperpolarization, is much larger than can be reproduced by this simple model.

These limitations of the present model can be overcome by a relatively simple

extension of the model: adding a third state to the 1, 2 subunit, so that it has states 1, 2, and 3. The channel would now be open only if this subunit were in the 3 state and the A,B subunit in the B state. To produce a rising phase in the gating current, charge moved in the new $1 \leftrightarrow 2$ transition would be smaller and slower than charge moved in the $2 \leftrightarrow 3$ transition. If the voltage over which the charge for these transitions is distributed includes both negative potentials (say, a midpoint near -45 or -50 mV for the $1 \leftrightarrow 2$ transition) and relatively positive voltages (say, -25 for the $2 \leftrightarrow 3$ transition), then the large separation between Q_{rel} and f_{open} will be preserved and would more closely reproduce the data. This modification will also produce a more sigmoid time course of the ionic current due to the time delay added by the $1 \leftrightarrow 2$ transition. Since the $1 \leftrightarrow 2$ transition would occur at relatively negative potentials, the magnitude of the Cole-Moore shift would be increased.

We do not yet have sufficient data on gating current OFF time constants and ionic current tails to include these in the simple model. Not only will such data be necessary for making the model more complete, but they also represent tests for the adequacy of this model.

The simple model presented here and the suggested extension make a particular prediction concerning the channel time constants that is shared by all models with independent subunits. For the simple model, three channel time constants are expected with the following values: τ_{12}, τ_{AB}, and $(\tau_{12} + \tau_{AB})/(\tau_{AB}\tau_{12})$. That is, the fastest time constant is the reciprocal sum of the other two. It is difficult to test this prediction with K channel gating currents because of the noise associated with measuring these relatively small currents and the way in which the amount and kinetics of charge movement weight the amplitude terms (Eq. 8). It may be possible to test this prediction with ionic currents if two problems can be resolved. The first is to prevent distortion of the ionic channel currents by K^+ accumulation in the periaxonal space. Our use of external solutions with an elevated concentration of K^+ reduces, but does not eliminate, the effects of accumulation. The second problem is the general difficulty of resolving several exponential components in data that contain noise. This problem is exacerbated by the presence of many components with similar time constants.

Little is known of the biochemical properties of K channels. In particular it is not known whether these proteins consist of one large polypeptide like the eel Na channel or if they are made up of several subunits like acetylcholine receptor channels. However, the recent discovery (Timpe et al., 1987) that a single (small) mRNA species is sufficient to allow functional expression of the inactivating A-type K channel suggests that this type of K channel may be a multimeric protein. Perhaps this result and the success of our subunit model in reproducing K channel function will stimulate the design of experiments to further test the applicability of this model.

We thank Dr. Gerry Oxford for suggesting the use of phloretin and for providing unpublished data, and Dr. Ruth Anne Eatock for comments on the manuscript. We are grateful to the Director and staff of the Marine Biological Laboratory for their assistance. We also thank Gerry Harris and Martin Gira for construction of the recording apparatus and voltage clamp circuity, and John Young of Scientific Associates for help with the data acquisition system.

This work was supported by U.S. Public Health Service grant NS-14138.

Original version received 21 March 1988 and accepted version received 1 August 1988.

REFERENCES

Adelman, W. J., Jr., Y. Palti, and J. P. Senft. 1973. Potassium ion accumulation in a periaxonal space and its effect on the measurement of membrane potassium ion conductance. *Journal of Membrane Biology.* 13:387–410.

Almers, W., and C. M. Armstrong. 1980. Survival of K^+ permeability and gating currents in squid axons perfused with K^+-free media. *Journal of General Physiology.* 75:61–78.

Armstrong, C. M., and F. Bezanilla. 1977. Inactivation of the sodium channel. II. Gating current experiments. *Journal of General Physiology.* 70:567–590.

Begenisich, T., and C. Lynch. 1974. Effects of internal divalent cations on voltage-clamped squid axons. *Journal of General Physiology.* 63:675–689.

Bezanilla, F., and C. M. Armstrong. 1974. Gating currents of the sodium channels: Three ways to block them. *Science.* 183:753–754.

Bezanilla, F., and C. M. Armstrong. 1977. Inactivation of the sodium channel. I. Sodium current experiments. *Journal of General Physiology.* 70:549–566.

Bezanilla, F., M. M. White, and R. E. Taylor. 1982. Gating currents associated with potassium channel activation. *Nature.* 296:657-660.

Busath, D., and T. Begenisich. 1982. Unidirectional sodium and potassium fluxes through the sodium channel of squid giant axons. *Biophysical Journal.* 40:41–49.

Caceci, M. S., and W. P. Cacheris. 1984. Fitting curves to data. *Byte.* 9:340–362.

Chandler, W. K., and H. Meves. 1965. Voltage clamp experiments on internally perfused giant axons. *Journal of Physiology.* 180:788–836.

Chandler, W. K., and H. Meves. 1970. Sodium and potassium currents in squid axons perfused with fluoride solutions. *Journal of Physiology.* 211:623-652.

Cole, K. S., and J. W. Moore. 1960. Potassium ion current in the squid giant axon: dynamic characteristic. *Biophysical Journal.* 1:1-14.

Conner, J. A., and C. F. Stevens. 1971. Inward and delayed outward membrane currents in isolated neural somata under voltage clamp. *Journal of Physiology.* 213:1–19.

Frankenhaeuser, B., and A. L. Hodgkin. 1956. The after-effects of impulses in the giant nerve fibres of *Loligo*. *Journal of Physiology.* 131:341–376.

Gilly, W. F., and C. M. Armstrong. 1980. Gating current and potassium channels in the giant axon of the squid. *Biophysical Journal.* 29:485–492.

Gilly, W. F., and C. M. Armstrong. 1982. Divalent cations and the activation kinetics of potassium channels in squid giant axons. *Journal of General Physiology.* 79:965–996.

Hodgkin, A. L., and A. F. Huxley. 1952*a*. The components of membrane conductance in the giant axon of *Loligo*. *Journal of Physiology.* 116:473–496.

Hodgkin, A. L., and A. F. Huxley. 1952*b*. A quantitative description of membrane current and its application to conduction and excitation in nerve. *Journal of Physiology.* 117:500–544.

Noble, D., and R. W. Tsien. 1969. Outward membrane currents activated in the plateau range of potentials in cardiac Purkinje fibres. *Journal of Physiology.* 200:205–231.

Palti, Y., G. Ganot, and R. Stampfli. 1976. Effect of conditioning potential on potassium current kinetics in the frog node. *Biophysical Journal.* 16:261–273.

Sillén, L. 1964. Stability constants of metal-ion complexes. London Chemical Society, London.

Spires, S., and T. Begenisich. 1985. Evidence for the presence of histidine on the external surface of the potassium channel and its involvement in channel gating. *Biophysical Journal.* 47:220*a*. (Abstr.)

Spires, S., and T. Begenisich. 1987. Important amino acids on the external surface of potassium channels. *Biophysical Journal.* 51:547*a*. (Abstr.)

Strichartz, G. R., G. S. Oxford, and F. Ramon. 1980. Effects of the dipolar form of phloretin on potassium conductance in squid giant axons. *Biophysical Journal.* 31:229–246.

Tasaki, I., I. Singer, and T. Takenaka. 1965. Effects of internal and external ionic environment on excitability of squid axon. A macromolecular approach. *Journal of General Physiology.* 48:1095–1123.

Timpe, L. C., T. L. Schwarz, B. L. Tempel, D. M. Papazian, Y. N. Jan, and L. Y. Jan. 1987. Expression of functional potassium channels from *Shaker* cDNA in *Xenopus* oocytes. *Nature.* 331:143–145.

Wagoner, P. K., and G. S. Oxford. 1987. Cation permeability through the voltage-dependent potassium channel in the squid axon. Characteristics and mechanisms. *Journal of General Physiology.* 90:261–290.

White, M. M., and F. Bezanilla. 1985. Activation of squid axon K^+ channels: Ionic and gating current studies. *Journal of General Physiology.* 85:539–554.